Applied Catalysis B: Environmental 215 (2017) 18–27

Contents lists available at ScienceDirect

Applied Catalysis B: Environmental

journal homepage: www.elsevier.com/locate/apcatb

Hydrophobic Pd nanocatalysts for one-pot and high-yield production of liquid furanic biofuels at low temperatures

Hu Li[a,b], Wenfeng Zhao[b], Zhen Fang[a,*]

[a] Biomass Group, College of Engineering, Nanjing Agricultural University, 40 Dianjiangtai Road, Nanjing, Jiangsu 210031, China
[b] State-Local Joint Engineering Laboratory for Comprehensive Utilization of Biomass, Center for R&D of Fine Chemicals, Guizhou University, Guiyang 550025, China

ARTICLE INFO

Article history:
Received 9 April 2017
Received in revised form 10 May 2017
Accepted 12 May 2017
Available online 18 May 2017

Keywords:
Biomass conversion
Liquid biofuel
Single-step process
Isotopic study
Pd nanocatalyst

ABSTRACT

Liquid furanic hydrocarbons, a class of biomass-based fuels and chemicals, are typically required to achieve moderate product selectivity and yield under harsh conditions (e.g., high temperature and H_2 pressure) involving multi-step processes over different catalysts. In this study, a single-step catalytic process was developed for direct conversion of various saccharides to furanic biofuels such as 2,5-dimethylfuran and 2-methylfuran with high yields (>95%) at 110–130 °C. The negatively charged hydride (H^-) of readily available polymethylhydrosiloxane (PMHS) acting as green H-donor over hydrophobic Pd nanoparticles did not obstruct upstream reactions (e.g., hydrolysis, isomerization and dehydration) for the *in situ* formation of furanic aldehydes/alcohols from sugars, and could selectively facilitate the subsequent hydrodeoxygenation of carbonyl and hydroxyl groups other than the furanic ring in one pot, as clarified by deuterium-labeling study. Importantly, the unreduced Pd(II) nanocatalysts also exhibited comparable performance in the selective hydrodeoxygenation reaction. Moreover, the catalytic strategy was extended to various carboxides for quantitative production of corresponding furanic/aromatic hydrocarbons at room temperature that were more pronounced than previously reported results, and the optimal Pd/MIL-53(Al) coated with polydimethylsiloxane (Pd/MIL-53(Al)-P) was highly stable with little deactivation and Pd leaching for at least five consecutive cycles.

1. Introduction

Direct valorization of biomass to biofuels and chemicals is of great interest to alleviate the reliance on fossil energy resources [1,2]. Catalytic conversion of biomass components (e.g., cellulose, hemicellulose, lignin and their derivatives) to liquid hydrocarbon fuels has been illustrated to be one of interesting approaches for advanced biofuels production [3,4]. However, these feedstocks are highly oxygenated with different functionalities, and oxygen removal reactions such as dehydration, hydrogenation and hydrodeoxygenation under relatively harsh conditions are required [5,6]. As a result, the catalytic systems having high selectivity toward hydrocarbons (especially furanic ones) have been pursued for decades, but with limited progress. For example, 2,5-dimethylfuran (DMF) is an extremely promising biomass-derived liquid fuel [7], and the most frequently employed catalytic processes for producing DMF are implemented at reaction temperatures of around 200 °C and high H_2 presures by hydrodeoxygenation of 5-hydroxymethylfurfural (HMF), a platform molecule derived from cellulose [8]. Unfortunately, a complicated two-step process involving the interval separation of in situ formed HMF catalyzed by an acid and mono-/bimetal in sequence is likely essential to reduce the formation of byproducts, when more abundant and easily available hexoses are used as substrates for DMF production [9,10]. Therefore, the development of new catalytic systems to enable the efficient production of furanic hydrocarbons directly from saccharides is urgently necessary.

Metal organic frameworks (MOFs), a class of porous and crystalline materials with larger pore volumes and higher surface areas than zeolites and even silicas, are very appropriate in heterogeneous catalysis [11]. The large flexibility in the composition endows the preparation of MOFs with anticipated structures and properties [12]. As solid supports, MOFs allow easy recovery of the occluded metal nanoparticles (NPs) and are helpful to stabilize the guest by the confinement, geometric restriction, and metal-support interactions [11]. Noble metal NPs are quite active in hydrogenation and hydrodeoxygenation reactions, while harsh conditions typically

* Corresponding author.
E-mail addresses: zhenfang@njau.edu.cn, zhen.fang@mail.mcgill.ca (Z. Fang).
URL: http://biomass-group.njau.edu.cn/ (Z. Fang).

http://dx.doi.org/10.1016/j.apcatb.2017.05.039
0926-3373/

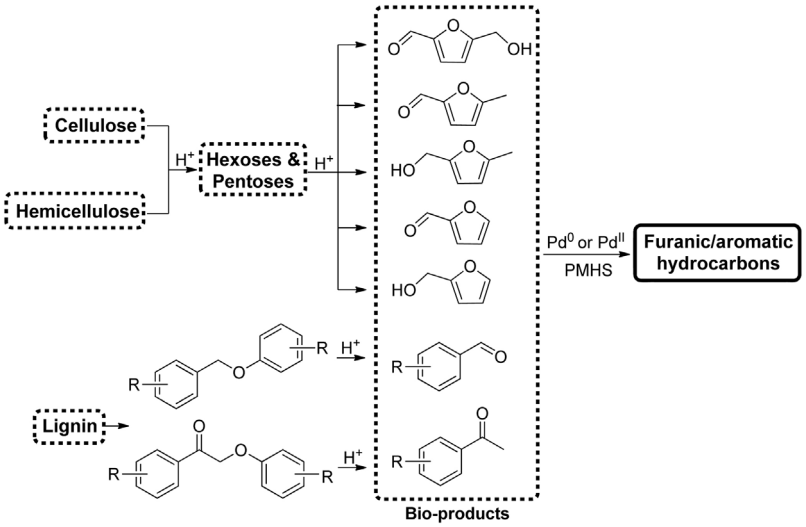

Scheme 1. Direct production of furanic/aromatic hydrocarbons from biomass derivatives.

lead to the formation of byproducts (e.g., humins and overhydrogenated compounds), thus lowering the yields of desired molecules [13]. In addition, the NPs may be agglomerated or leached once liberating from the constraint of MOFs during reactions [14], which can be impeded by the hydrophobic modification of the porous surface [15]. However, to the best of our knowledge, no study has been made on enhancing the catalytic performance of metal NPs/MOFs by the increment of surface hydrophobicity for the mild production of furanic biofuels from biomass derivatives via a single-step process.

In the present study, Pd NPs immobilized on typical MOFs with increased hydrophobicity were simply realized by chemical vapor deposition, and explored to be highly efficient and robust for the domino transformation of carbohydrates and a variety of biomass-derived products to corresponding hydrocarbons via a single-step process (Scheme 1), without intermediates separation/purification in an alcoholic medium using a liquid H-donor polymethylhydrosiloxane (PMHS) that is a water/air insensitive, non-toxic, and inexpensive coproduct of the silicone industry [16]. Near quantitative yields of furanic/aromatic hydrocarbons (e.g., DMF) were obtained directly from various biomass derivatives in one pot under unprecedentedly benign reaction conditions (as low as room temperature). More importantly, the unreduced Pd(II)/MOFs also exhibited comparable catalytic activity in the selective hydrodeoxygenation of carbonyl groups without significant influence on the furanic ring of biomass-derived compounds. In addition, deuterium isotope labeling experiments were conducted to investigate the reaction pathway.

2. Materials and methods

2.1. Materials

Fructose (99%), glucose (>99.5%), xylose (>99%), sucrose (>99%), inulin (>99%), cellulose (particle size 25 μm), 5-hydroxymethylfurfural (HMF, >99%), 5-methylfurfural (98%), furfural (99%), furfuryl alcohol (98%), benzaldehyde (>98%), acetophenone (>99%), activated charcoal (>99.9%), $Pd(NO_3)_2$ (>99.9%), H_2PtCl_4 (>99.9%), $RuCl_3$ (99%), $Ni(NO_3)_2$ (98%), $Co(NO_3)_2$ (99%), ZrO_2 (>99.99%), Al_2O_3 (99.9%), poly(methylhydrosiloxane) (PMHS), 2-butanol (>99.0%), 2-propanol (99.5%), and *n*-hexanol (>99%) were purchased from Aladdin Industrial Inc. (Shanghai). 5-Methyfurfuryl alcohol (99.9%) and polydimethylsiloxane (PDMS) were bought from Acros Organics Inc. (Geel, Belgium). Methanol-d_4 (CD_3OD, 99.8 atom% D) and chloroform-d_1 ($CDCl_3$, 99.6 atom% D) were purchased from Alfa Aesar Inc. (Shanghai). 2,5-Dimethyltetrahydrofuran (DTHF, >98.0%), *n*-butyl levulinate (BL, >98.0%), and chlorosulfonic acid (97%) were bought from TCI Inc. (Shanghai). Diphenyl (silane-d_2) (97 atom% D) was purchased from Sigma-Aldrich Co. LLC (Shanghai). TiO_2 (99%) was bought from Innochem Inc. (Beijing). 2,5-Dimethylfuran (DMF >98%), *n*-butanol (AR), ethanol (AR), methanol (AR), *n*-propanol (AR), dimethyl formamide (99.8%), and acetone (AR) were bought from J&K Scientific Ltd. (Beijing).

2.2. Catalyst preparation

The typical metal-organic frameworks including MIL-101(Cr), MIL-53(Al), and UiO-66(Zr) were synthesized, according to previously reported procedures [17–19]. For the immobilization of 3 wt% Pd(II) onto a solid support (i.e., MIL-101(Cr), MIL-53(Al), UiO-66(Zr), ZrO_2, TiO_2, C, or Al_2O_3), an impregnation method was adopted. In a general process, to a solution of 16 mg $Pd(NO_3)_2$ dissolved in 1.2 mL deionized water, 0.25 g solid support was added. The resulting mixture was treated by ultrasound for 30 min, and then stirred at room temperature for 24 h. Upon completion, the precipitates were collected by centrifugation, followed by washing with *N,N*-dimethyl formamide for three times to remove water in the framework and loosely supported Pd species, and then dried at 90 °C under vacuum condition overnight to give the supported Pd(II) catalysts denoted as Pd^{II}/M (M = MIL-101(Cr), MIL-53(Al), UiO-66(Zr), ZrO_2, TiO_2, C, or Al_2O_3).

To prepare the reduced Pd nanoparticles (NPs), the resulting supported Pd(II) catalysts were placed into a muffle and programmatically heated to 200 °C for 2 h (with a heating ramp of 10 °C/min) in the atmosphere of 10% H_2/Ar (with a flow rate of 30 cm^3/min). The target catalyst was denoted as Pd/M (M = MIL-101(Cr), MIL-53(Al), UiO-66(Zr), ZrO_2, TiO_2, C, or Al_2O_3).

For the preparation of hydrophobic MIL-53(Al)-P, Pd/MIL-53(Al)-P and Pd^{II}/MIL-53(Al)-P catalysts, a chemical vapor deposition approach was used. In detail, 20 mg of MIL-53(Al), Pd/MIL-53(Al) or Pd^{II}/MIL-53(Al) was evenly dispersed into a watch glass, and then tranferred into an autoclave fitted with Teflon lining that containing some PDMS. The sealed reactor was subsequently placed into an oven and thermally treated at 205 °C for 30 min to coat a layer of hydrophobic PDMS.

2.3. Catalyst characterization

The contents of metals were determined by ICP-OES (inductively coupled plasma-optical emission spectrometer) on an Optima 5300 DV instrument (PerkinElmer Inc., Waltham, MA). BET (Brunauer-Emmett-Teller) surface areas of the porous materials were determined from nitrogen physisorption measurements at liquid nitrogen temperature on a Micromeritics ASAP 2010 instrument (Tristar II 3020, Norcross, GA). XRD (X-ray diffraction) patterns were recorded with D/max-TTR III X-ray powder diffractometer (Rigaku International Corp., Tokyo) using Cu Kα radiation source. Scanning transmission electron microscope and high-angle annular dark/bright-field (STEM-HAADF/BF) imaging were acquired with an aberration corrected FEI TECNAI G2 F30 S-TWIN (S)TEM (Hillsboro, OR) operating at 300 kV, along with the capability of taking energy dispersive X-ray (EDX) spectra. FT-IR spectra were recorded on a Perkin-Elmer 1710 spectrometer at ambient conditions in KBr disks. The contact angle of a water droplet was measured using a SORPTION ANALYZER of MB-300G (VTI Corporation, Hialeah, FL) at 25 °C. XPS (X-ray photoelectron spectroscopy) measurements were recorded using a Physical Electronics Quantum 2000 Scanning ESCA Microprobe (Physical Electronics Inc., PHI, MN) equipped with a monochromatic AlKa anode. H_2-TPR (temperature programmed reduction) was conducted on an AutoChem 2920 chemisorption analyzer (Micromeritics Instrument Corp., Norcross, GA) to assess the reduction properties of catalysts.

2.4. Reaction procedures

The reactions with various substrates were conducted in a 15 mL Ace glass tube. In a typical procedure, 3 wt% substrate (120 mg) in 4 g *n*-BuOH (5 mL), 6 mol% chlorobenzene (4.5 μL), 1 mol% metal in the catalyst (~14 mg) and 8 equiv. H^- of PMHS (0.38 g) were added into the tube, which was magnetically stirred at 500 rpm for a specific reaction time. The time zero was defined as the tube was placed into an oil bath that was preheated to 90–130 °C or at room temperature (25 °C). Upon completion, liquid products in *n*-BuOH after centrifugation and filtration were quantitatively analyzed by HPLC and GC. For more clear illustration, a schematic diagram of the experimental set-up was provided in Scheme S1 (Supporting Information).

For deuterium-labeling study, GC–MS spectra of reaction mixtures starting from HMF were performed in the deuterium solvent methanol-d_4 or chloroform-d_1 with D-labeled silicon: diphenyl(silane-d_2).

2.5. Catalyst recycle study

After each cycle of reactions, the solid catalyst in the mixture was recovered by centrifugation, and washed with ethanol and acetone for 5 times, dried at 100 °C under vacuum condition for 5 h, and directly employed for the next run.

2.6. Product analysis

GC–MS (Agilent 6890N GC/5973 MS, Santa Clara, CA) was used to identify liquid products and major by-products. The concentrations of sugars and furanic aldehydes or alcohols were determined by HPLC (LC-20A, Shimadzu, Kyoto) fitted with an Aminex HPX-87H column (Bio-Rad, Richmond, CA) and a refractive index (RI) detector as well as an ultraviolet (UV) detector at 280 nm. The reaction mixtures (especially for quantification of furanic/aromatic hydrocarbons) were also analyzed on GC (Agilent 7890B) with an HP-5 column (30 m × 0.320 mm × 0.25 μm) and a flame ionization detector using naphthalene as internal standard and referring to the standard curves (with $R^2 > 0.997$) made from commercial samples.

3. Results and discussion

3.1. Catalyst characterization

XRD patterns of MIL-53(Al), Pd^{II}/MIL-53(Al) and Pd/MIL-53(Al) demonstrate the intact crystalline structure of MIL-53(Al) after encapsulation of Pd(II) or Pd nanoparticles (NPs; Fig. 1A). In the case of Pd/MIL-53(Al)-P, a range of wide and low bands were observed, indicating the successful coating of PDMS onto the surface of Pd/MIL-53(Al). The structure of other MOFs (i.e., MIL-101(Cr) and UiO-66(Zr)) to immobilize Pd NPs was also examined, which was found to be well retentive, as illustrated by XRD patterns (Fig. S1, Supporting Information). However, it was worth noting that metal oxides (especially Al_2O_3 and ZrO_2) showed slightly changed crystalline structure before and after Pd(II) reduction at 200 °C for 2 h, implying the serious aggregation of Pd species and the relatively low stability of metal oxides. Fig. 1 B shows that MIL-53(Al), Pd/MIL-53(Al), and Pd/MIL-53(Al)-P have abundant micro- and mesopores bearing a mean pore diameter of 2.4–3.0 nm (Table 1). However, the BET surface area of MIL-53(Al) gradually decreased from 1728 to 1165 and 952 m^2/g together with pore volume reducing from 0.72 to 0.58 and 0.54 cm^3/g after the successive deposition of Pd species and PDMS (Table 1). To our delight, the texture properties of Pd NPs supported on MOFs including MIL-53(Al), MIL-101(Cr) and UiO-66(Zr) were all superior to those on metal oxides (e.g., Al_2O_3, ZrO_2 and TiO_2) and carbon (Table 1, Fig. S2, Supporting Information).

ICP analysis shows that the Pd loading for all the catalysts was around 3 wt%, and their acid contents (0.09-1.04 mmol/g) and Pd particles diameters (1.8-9.5 nm) were found to closely depend on the metal species of solid supports, as determined by NH_3-TPD (Table 1). Fig. 1C manifests the hydrophobicity of Pd/MIL-53(Al) could be significantly increased (with water contact angle increasing from 24° to 135°) by coating a thin layer of PDMS via a simple chemical vapor deposition approach. As demonstrated by FT-IR spectra (Fig. 1D), the emergence of additional stretching vibrations of C—H at ~2900 cm^{-1} and Si—O—Si at ~1000 cm^{-1} further confirms the successful introduction of PDMS.

3.2. Direct production of DMF from fructose with different Pd^0 catalysts

Our study began with the one-pot, single-step conversion of fructose to the biofuel DMF at 110 °C on Pd NPs with different supports in *n*-butanol, a bio-based solvent. The activity of Pd NPs was observed to greatly depend on the supports (Fig. 2A), and Pd/MIL-53(Al) stood out affording a good DMF yield of 78% with 93% fructose conversion after only 75 min. Other metals (Ru, Pt, Ni and Co) were also tested, but exhibited relatively poor performance (0–22% DMF yields; Table S1, entries 1–5, Supporting Information) than Pd/MIL-53(Al) and other Pd NPs. In addition, the parent supports did not produce any DMF but HMF from fructose under identical conditions (Table S1, entries 6–13). Based on these results, the co-existence of Pd species and MIL-53(Al) can be envisaged to be essential for achieving a high yield of DMF. Therefore, the effect of support acidity and Pd size on the activity of different catalysts was further investigated (Fig. 2B). TOF (turnover frequency) values were observed to be positively correlated with the size of Pd NPs but not closely relevant to the acidity of solid supports. As an exception, Pd/MIL-101(Cr) with the lowest Pd size (1.8 nm) gave a relatively lower TOF (109 h^{-1}) and DMF yield (56%), which can be ascribed to the limited access of reagents to active sites due to the smallest average pore diameters of MIL-101(Cr) possessing abundant micro-

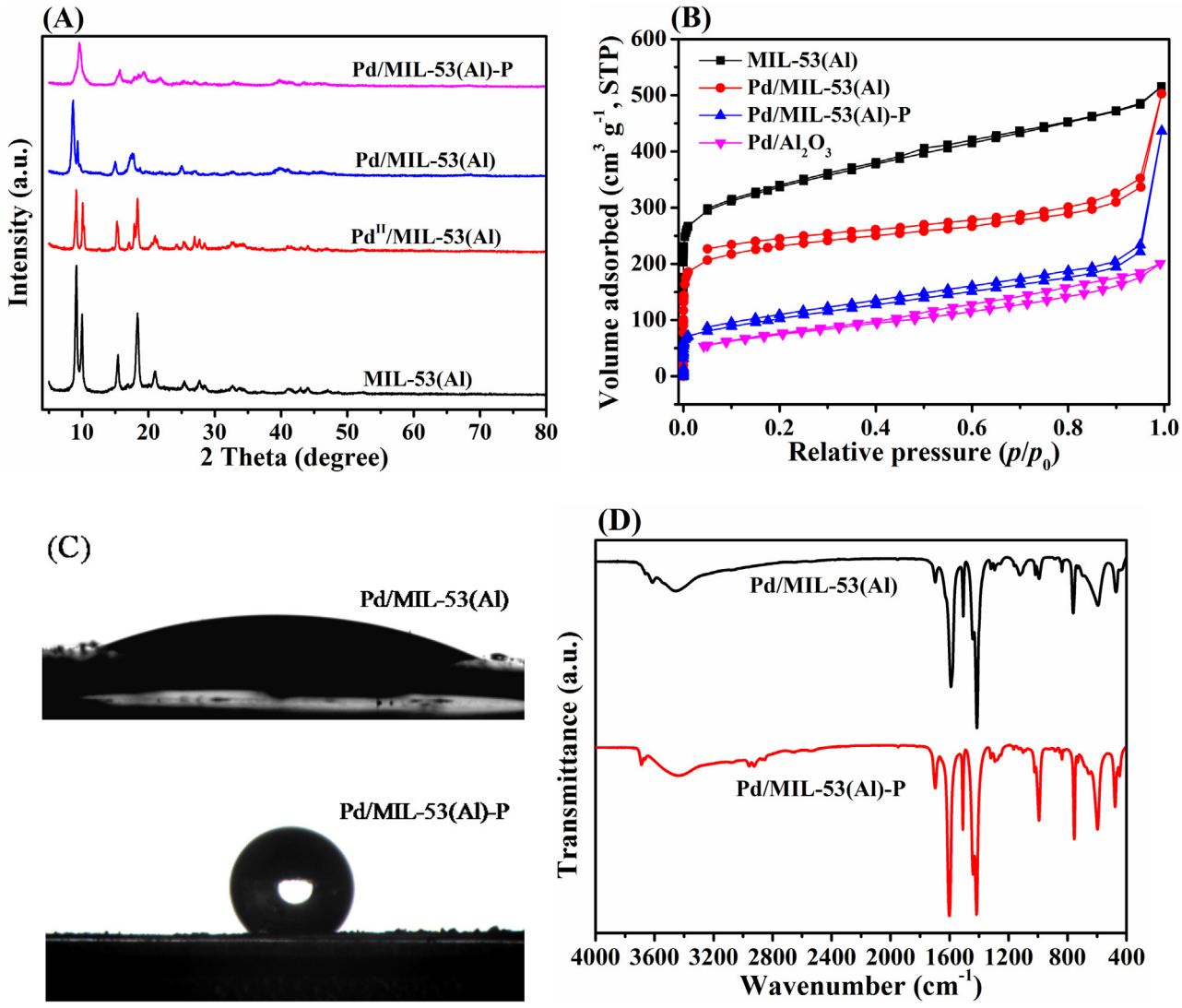

Fig 1. (A) XRD patterns, (B) nitrogen adsorption-desorption isotherms, (C) water contact angles, and (D) FT-IR spectra of different Pd-containing catalysts.

Table 1
Physicochemical properties of different catalysts.

Catalyst	S_{BET} (m^2/g)[a]	V_{pore} (cm^3/g)[b]	D_{mean} (nm)[c]	Pd loading (wt%)[d]	Acidity (mmol/g)[e]	Pd particles diameter (nm)[f]
MIL-53(Al)	1728	0.72	2.8	–	0.42	–
Pd/MIL-53(Al)	1165	0.58	3.0	3.1	0.35	2.6
Pd/MIL-53(Al)-P	952	0.54	2.4	2.8	0.26	2.2
Pd/Al_2O_3	266	0.23	3.5	3.0	0.27	3.7
MIL-101(Cr)	2842	1.01	1.9	–	0.87	–
Pd/MIL-101(Cr)	2548	0.98	2.3	3.3	0.69	1.8
Pd/MIL-101(Cr)-SO_3H	1854	0.85	2.7	2.9	1.04	2.4
UiO-66(Zr)	1571	0.68	3.7	–	0.65	–
Pd/UiO-66(Zr)	1085	0.62	4.3	3.2	0.43	3.5
Pd/ZrO_2	35	0.03	3.4	2.7	0.13	9.5
Pd/TiO_2	79	0.12	6.1	2.9	0.18	6.6
Pd/C	807	0.81	4.0	3.2	0.09	4.7

[a] BET surface area was obtained from N_2 adsorption isotherm.
[b] Volume of pores was estimated from BJH Adsorption cumulative volume of pores.
[c] Average pore size was estimated from the adsorption average pore diameter.
[d] Pd loading was determined by IPC analysis.
[e] Acidity of the catalyst was determined with NH_3-TPD with a programmed temperature: heating from 50 to 300 °C at a rate of 10 °C/min and then kept at 300 °C for 60 min gas desorption.
[f] Pd particles diameter was estimated from HR-TEM.

pores and tight Pd encapsulation. Furthermore, the inferior activity of Pd/MIL-101(Cr)-SO_3H by using either PMHS or H_2 as H-donor to the pristine Pd/MIL-101(Cr) under comparable conditions (Table S1, entries 14–15) indicates the non-dominant role of acidic support, to some extent. In this scenario, it can be speculated that the enhanced performance of Pd NPs available to substrates are most

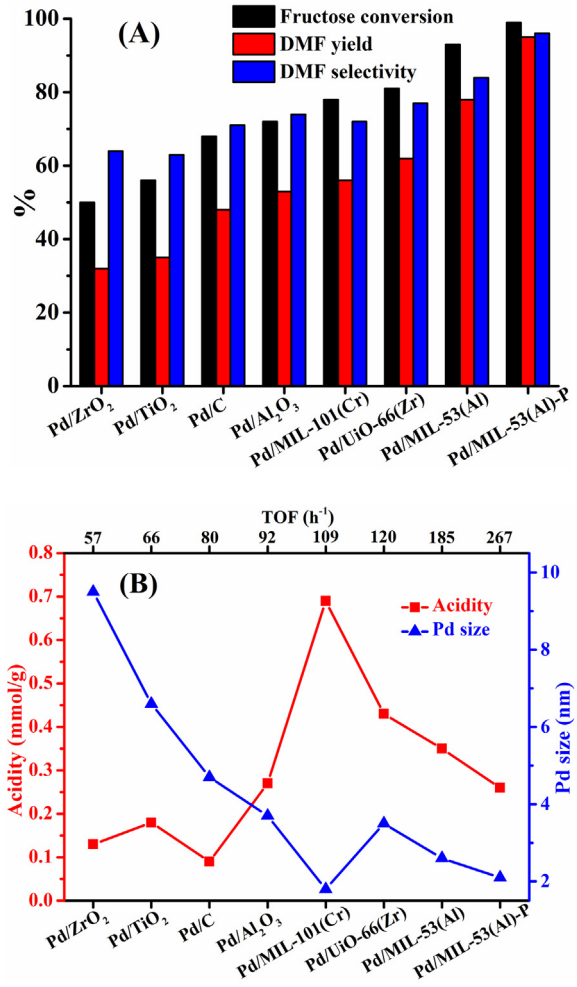

Fig. 2. (A) Production of DMF from fructose via a single-step process on Pd NPs with different supports and (B) Effect of support acidity and Pd size on TOF values at 110 °C [Reaction conditions: 3 wt% fructose, 4 g *n*-BuOH (5 mL), 8 equiv. H^- of PMHS, 1 mol% Pd, 6 mol% chlorobenzene (4.5 μL), and 75 min; TOF = (mole of converted fructose)/(mole of Pd NPs × time), which was determined at fructose conversion of ~20%.].

likely to be acquired via dipolar Coulombic interactions with metal nodes and π interactions with organic phenyl linkers of MOFs [11].

As discussed in the context, the resulting hydrophobic composites (i.e., Pd/MIL-53(Al)-P) retained accessibility (Table 1) and crystallinity of MOFs (Fig. 1A), which is in accordance with previous reports [20,21]. Remarkably, an excellent DMF yield of 95% at complete fructose conversion was attained over Pd/MIL-53(Al)-P, with a TOF of 267 h^{-1} which is about 1.5 and 2–5 times higher than that of the pristine Pd/MIL-53(Al) and other Pd NPs, respectively (Fig. 2). This fact indicates that the hydrophobic surface of Pd/MIL-53(Al)-P matching the wettability of PMHS to execute hydride transfer and chlorobenzene to release HCl during reactions may contribute to the pronounced catalytic performance. Moreover, the relatively high efficiency in long-chain alcohols further verifies the significance of appropriate wettability for DMF production (Table 2). It should be noted that the superior activity of primary alcohol compared to secondary counterpart (Table 2, entries 3–6) was possibly attributed to its relatively higher steric hindrance when reacting with PHMS, indicating the crucial role of alkoxide moiety of alcohols in liberating H^- from PHMS to facilitate the processes of hydrogenation and hydrodeoxygenation.

To elucidate the underlying reasons for such evident distinctions in activity before and after PDMS coating onto Pd/MIL-53(Al),

Table 2
Effect of solvent type on the direct conversion of fructose to DMF over Pd/MIL-53(Al)-P.

Entry	Solvent	Fructose conv. (%)	Product yield (%)			
			HMF	BL	DTHF	DMF
1	Methanol	93	4	7	2	71
2	Ethanol	96	6	5	1	79
3	*n*-Propanol	98	3	2	0	87
4	2-Propanol	92	5	3	1	80
5	*n*-Butanol	99	2	1	0	95
6	2-Butanol	95	1	1	1	82
7	*n*-Hexanol	97	<1	<1	0	90

Reaction conditions: 3 wt% fructose (120 mg), 4 g *n*-BuOH (5 mL), 8 equiv. H^- of PMHS (0.38 g), 1 mol% Pd (14 mg), and 6 mol% chlorobenzene (4.5 μL), 110 °C, and 75 min. HMF: 5-hydroxymethylfurfural; BL: *n*-butyl levulinate; DMF: 2,5-dimethylfuran; DTHF: 2,5-dimethyltetrahydrofuran.

HAABF-STEM images of these materials were examined (Fig. 3). Pd NPs in size of <5 nm were observed for both Pd/MIL-53(Al) and Pd/MIL-53(Al)-P, while the average Pd size of the latter (2.2 nm) decreased a little compared to the former (2.6 nm), which implies the possible interaction of the pristine catalyst with PDMS. Although a small quantity of Pd NPs had particle size larger than MIL-53(Al), the porous MOF could offer spatial restriction to the metal NPs in some degree [22].

Elemental mappings were further performed and clearly manifest that a number of Pd NPs are evenly dispersed on the supports, and the uniform distribution of Si with a little bit high intensity shows the stable encaptulation of PDMS (Figs. S3-S4, Supporting Information). XPS spectrum of Pd/MIL-53(Al)-P reveals a distinct signal for Si 2p (Fig. S5, Supporting Information), which confirms the successful coating of PDMS onto the Pd/MIL-53(Al) surface via cross connection [21]. Accordingly, the defects of PDMS coating can be assumed to facilitate the transportation of reactants and resultants during reactions. In addition, the XPS peak splitting of Pd 3d (Pd^0 at 334.8 to PdO_x species at 337.1 eV) in Pd/MIL-53(Al)-P (Fig. 4A) suggests the change in the electronic state of Pd NPs after PDMS coating [23,24], while the almost persistent XPS signals of Al 2p for both Pd NPs (Fig. 4B) demonstrate the high stability of MIL-53(Al) in the process of heat treatment for coating PDMS. Thus, besides the positive role of hydrophobic surface, the electronic state of Pd 3d that enabled the formation of Pd NPs in smaller size were most likely to promote the efficient production of DMF from fructose involving multiple reactions via a single-step process.

3.3. *Effect of reaction time, temperature and Pd dosage*

In order to comprehend the product distribution over 1 mol% Pd/MIL-53(Al)-P, the effect of reaction temperature and time was also investigated (Fig. 5). The rise of 90–130 °C significantly accelerated the reaction rate, and no more than 120 min was required to complete fructose conversion. HMF derived from fructose dehydration was observed to be the key intermediate for DMF production, which was relatively enriched at a low temperature of 90 °C in the early stage of 30–75 min. With the increase of reaction time and temperature, DMF was predominantly formed with some byproducts such as 2,5-dimethyltetrahydrofuran (DTHF) and *n*-butyl levulinate (BL) in total yields of 1–15% (Fig. 5). The reaction conducted at 110 °C was demonstrated to be favorable for the generation of DMF, and a high yield of 95% with few BL (1%) was obtained after 75 min. Remarkably, Pd NPs in a dosage as low as 0.2 mol% could also catalyze fructose being completely converted to DMF (85% yield) for a longer time of 120 min (Fig. S6, Supporting Information). These results illustrated the excellent performance of Pd/MIL-53(Al)-P in the selective production of DMF from fructose.

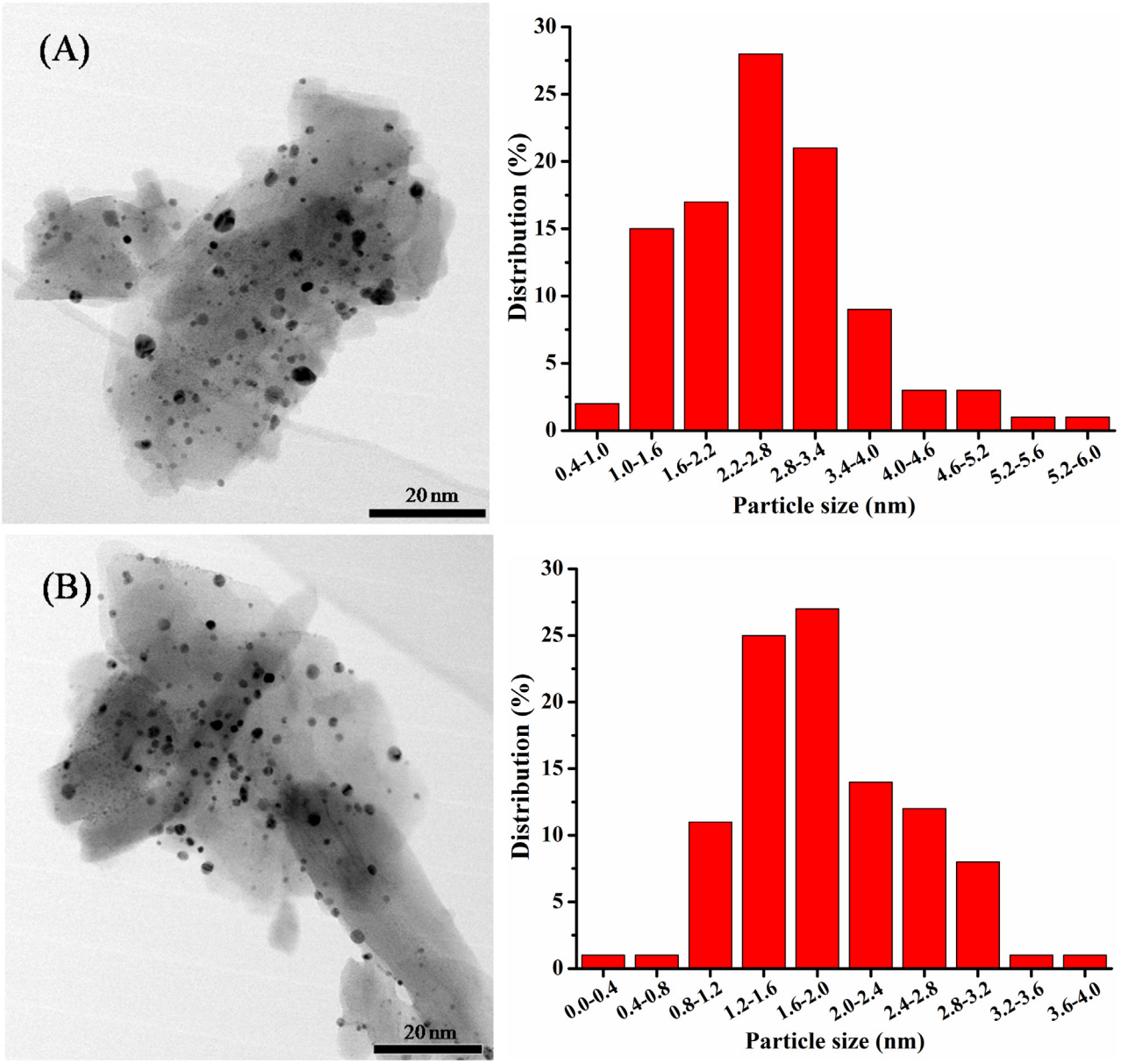

Fig. 3. HAABF-STEM images and Pd nanoparticle size distrinution of (A) Pd/MIL-53(Al) and (B) Pd/MIL-53(Al)-P.

3.4. Catalyst recycle study

As a heterogeneous protocol for potential practical application, the recyclability of Pd/MIL-53(Al)-P was studied under the optimized reaction conditions (Fig. 6). To our delight, the catalyst could be reused for five consecutive cycles without significant decrease in catalytic performance, although NH_3-TPD and TEM analyses of recycled Pd/MIL-53(Al)-P catalyst reveal the decrease in acidity (Fig. S7, Supporting Information) and the slight increase in the size of Pd NPs (from ~2.2 to 2.5 nm), respectively. These results confirmed that the acidic support did not directly affect fructose dehydration that might be mainly promoted by *in situ* formed HCl from chlorobenzene, as well as subsequent hydrodeoxygenation process with PMHS. Further, ICP analysis shows little leaching of Pd species into reaction solutions over multiple uses (< 0.2 ppm), with a catalyst recovery rate of around 93% after each cycle. These results indicate that the loss of the catalytic material during reactions may partially contribute to the slightly decreased activity in the fifth run. H_2-TPR profiles of different catalysts indicate the full reduction of Pd species at 200 °C (Fig. S8, Supporting Information). Nevertheless, a fraction of remained Pd^{II} (~337 eV binding energy) on the surface of fresh Pd/MIL-53(Al)-P was predominantly reduced to Pd^0 (~335 eV) after one cycle, as illustrated by Pd 3d XPS spectra in Fig. S9 (Supporting Information).

3.5. Direct production of DMF from fructose with different Pd^{II} catalysts

To verify whether Pd^{II} species was able to catalyze fructose-to-DMF conversion, the catalytic performance of Pd^{II} on different supports were examined (Fig. 7). It was interesting to note that all of these catalysts could produce DMF in moderate to good yields, wherein Pd^{II}/MIL-53(Al)-P exhibited the highest activity (up to 90% DMF yield) at 110 °C after 90 min. STEM images and Al, O & Pd elemental mappings of fresh and reused Pd^{II}/MIL-53(Al) catalysts unambiguously affirm the unnoticeable change in the size of Pd NPs and homogeneous dispersion of elements before and after reactions (Figs. S10–S12, Supporting Information). Unexpectedly, Pd^{II}

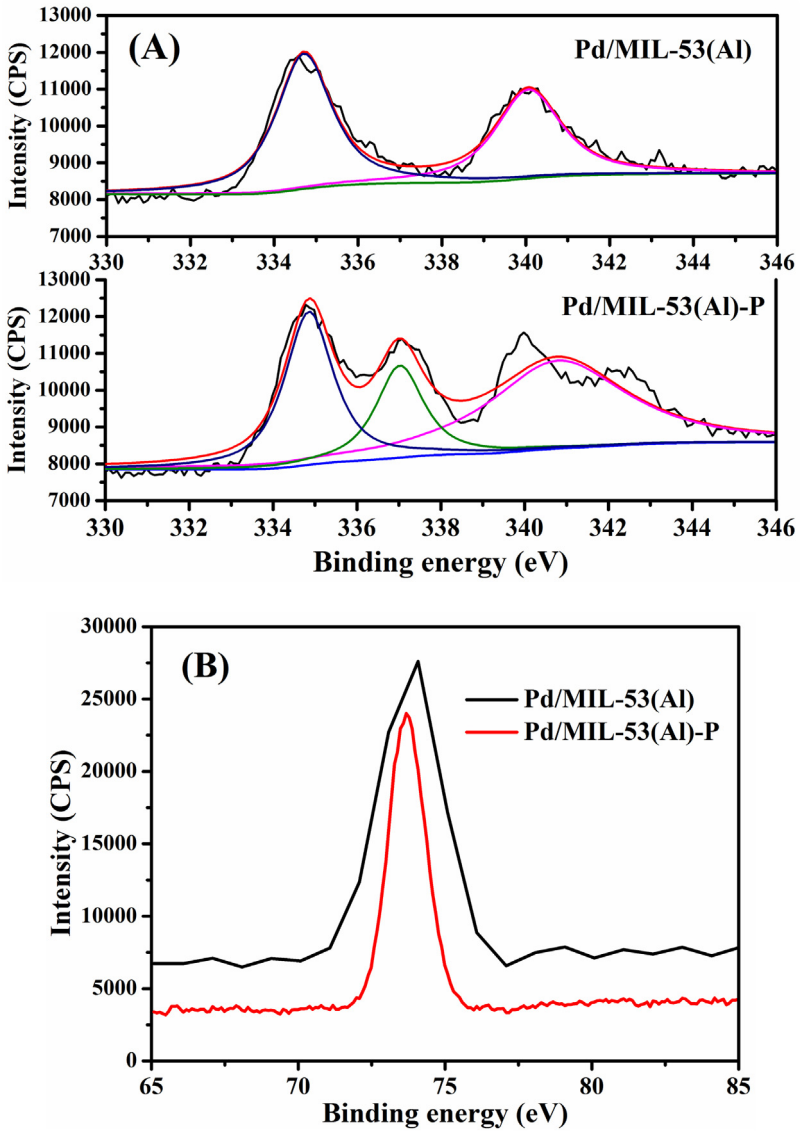

Fig. 4. (A) Pd 3d and (B) Al 2p XPS spectra for Pd/MIL-53(Al) and Pd/MIL-53(Al)-P.

Table 3
Catalytic production of different furanic/aromatic hydrocarbons from biomass derivatives with Pd/MIL-53(Al)-P.

Entry	Substrate	Product	Temp. (°C)	Time (min)	Conv. (%)	Yield (%)
1	Fructose	DMF	110	75	99	95
2	Glucose	DMF	130	120	95	54
3	Sucrose	DMF	110	150	100	73
4	Inulin	DMF	110	150	97	86
5	Cellulose[a]	DMF	130	180	–	32
6	Xylose	MF	130	120	93	45
7	HMF	DMF	25	150	100	99
8	5-Methylfurfural	DMF	25	120	100	>99
9	5-Methylfurfuryl alcohol	DMF	25	90	99	98
10	Furfural	MF	25	120	100	97
11	Furfuryl alcohol	MF	25	90	98	96
12	Benzaldehyde	Toluene	25	120	100	97
13	Acetophenone	Ethylbenzene	25	120	99	95

Reaction conditions: 3 wt% substrate, 4 g *n*-BuOH (5 mL), 8 equiv. H^- of PMHS, 1 mol% Pd, and 6 mol% chlorobenzene (4.5 μL).
[a] Ball-milled cellulose. DMF: 2,5-dimethylfuran; MF: 2-methylfuran.

(336.8 eV) was almost completely reduced to Pd^0 (334.6 eV) after reusing for one time (Fig. S13, Supporting Information), and a little enhanced DMF yield (92%) was achieved under identical reaction conditions over the reused Pd^{II}/MIL-53(Al) catalyst after one cycle. In this case, the Pd^0 species from either prereduction or *in situ* reduction of Pd^{II}, which is in close interaction with hydrophobic MIL-53(Al), can be concluded to be responsible for the pronounced performance.

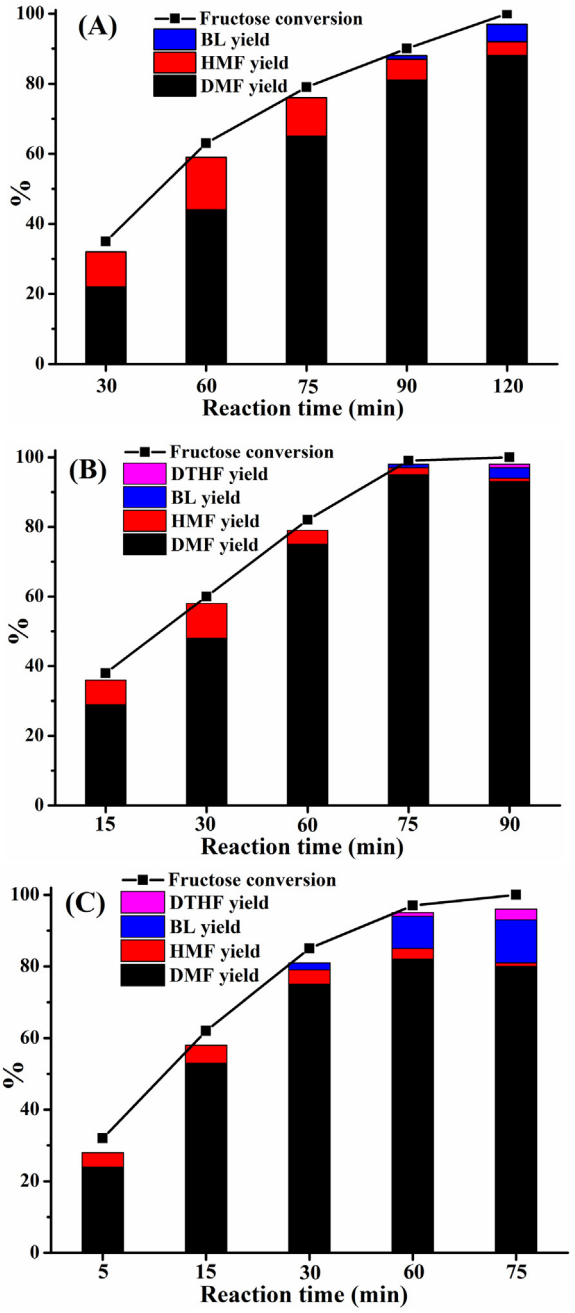

Fig. 5. Catalytic production of DMF from fructose with Pd/MIL-53(Al)-P by varying reaction time (5–120 min) at temperatures of (A) 90 °C, (B) 110 °C, and (C) 130 °C [Reaction conditions: 3 wt% fructose, 4 g *n*-BuOH (5 mL), 8 equiv. H^- of PMHS, 1 mol% Pd, and 6 mol% chlorobenzene (4.5 μL). DTHF: 2,5-dimethyltetrahydrofuran; BL: *n*-butyl levulinate; DMF: 2,5-dimethylfuran].

3.6. Production of different furanic/aromatic hydrocarbons from biomass derivatives

Encouraged by the outstanding catalytic performance of Pd/MIL-53(Al)-P in the single-step conversion of fructose to DMF under mild conditions, a variety of biomass-derived carbohydrates and simple bio-products were also used as substrates to produce corresponding furanic/aromatic hydrocarbons (Table 3). Unlike fructose (entry 1), glucose was more difficult to be converted to DMF with a moderate yield of 54%, and relatively harsh conditions (130 °C for 120 min) were required (entry 2). Gratifyingly, the production of DMF (up to 86% yield) from disaccharide (sucrose)

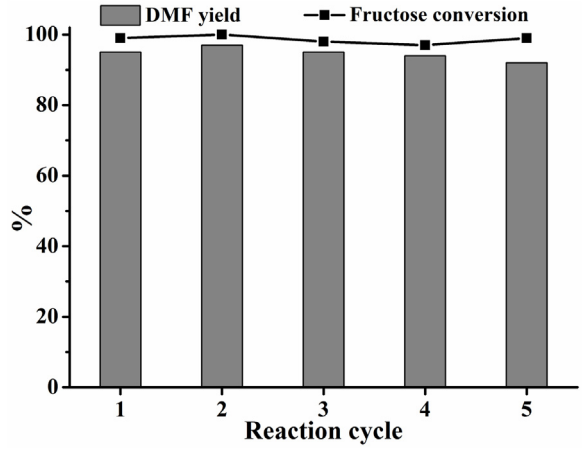

Fig. 6. Recycle study of Pd/MIL-53(Al)-P in single-step production of DMF from fructose [Reaction conditions: 3 wt% fructose, 4 g *n*-BuOH (5 mL), 8 equiv. H^- of PMHS, 1 mol% Pd, and 6 mol% chlorobenzene (4.5 μL), 110 °C, and 75 min].

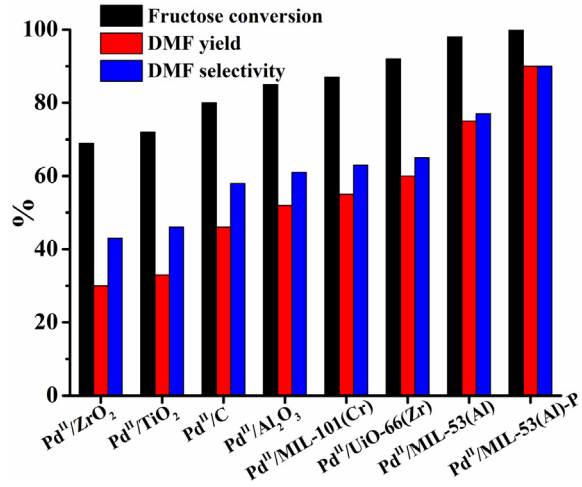

Fig. 7. Catalytic production of DMF from fructose with Pd^{II} on different supports via a single-step process at 110 °C [Reaction conditions: 3 wt% fructose, 4 g *n*-BuOH (5 mL), 8 equiv. H^- of PMHS, 1 mol% Pd, 6 mol% chlorobenzene (4.5 μL), and 90 min].

and polysaccharide (inulin and cellulose) was also achieved via a single-step process (entries 3–5). In addition to hexose sugars, the pentose xylose could also perform cascade dehydration and hydrodeoxygenation to give about 50% 2-methylfuran (MF; entry 6). More importantly, simple bio-products derived from saccharides and lignin were almost quantitatively tansformed into furanic and aromatic hydrocarbons at room temperature after 90–120 min (entries 7–13). These results clearly indicated the feasibility and universality of using Pd/MIL-53(Al)-P as bifunctional catalyst for the benign and facile production of different hydrocarbons from biomass derivatives. It was worthy noting that this simple catalytic system with milder reaction conditions showed more pronounced performance, compared to previously reported results (Table S2, Supporting Information) [25–31].

3.7. Proposed reaction mechanism

A controversy on the hydrogen source provided by the alcoholic solvent and/or PMHS is usually encountered, due to the occurrence of H/D exchange between PMHS and the deuterium protic solvent [32–34]. Therefore, GC–MS would be a better choice than ^{1}H NMR for product analysis. In connection to this, catalytic hydrodeoxygenation of HMF with Pd/MIL-53(Al)-P and PMHS

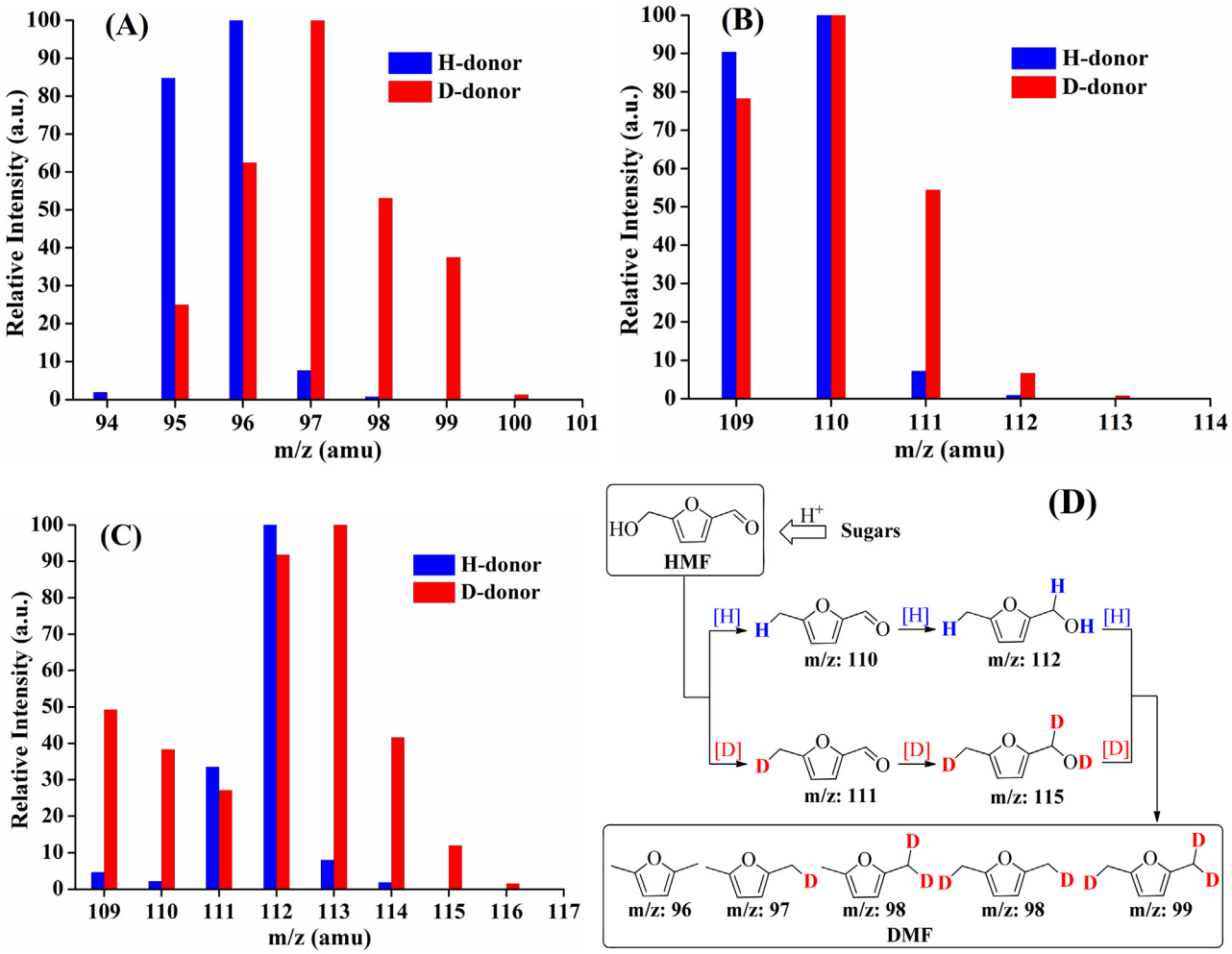

Fig. 8. Mass fragmentation analysis (all intensities scaled to 100%) of different products from HMF at room temperature for 1 h by using PMHS as H-donor and diphenyl (silane-d_2) as D-donor: (A) DMF, (B) 5-methylfurfural, and (C) 5-methylfurfuryl alcohol. (D) Schematic of reaction pathway for DMF production.

in CD_3OD at room temperature for 1 h gave DMF with +1, +2, +3 and +4 mass shifts (*m/z*, amu) from that in CH_3OH (Fig. S14 A-B, Supporting Information). To our delight, when $CDCl_3$ as solvent along with PMHS was used, there was no evident mass shift (Fig. S14C) except for the small signal caused by the natural isotope abundance of ^{13}C [35], indicating that PMHS was most likely to be the H-donor. The use of a counterpart diphenyl(silane-d_2) instead of PMHS in $CDCl_3$ for hydrodeoxygenation of HMF could afford DMF with 97–100 amu *m/z* in a much higher proportion to that of 96 amu *m/z* (Fig. 8A; Fig. S14 C–D), further confirming the predominant hydrogen-donating role of PMHS. In addition, 5-methylfurfural and 5-methylfurfuryl alcohol were found to be the major intermediates for producing DMF from HMF in $CDCl_3$, as demonstrated by employing PMHS and diphenyl(silane-d_2) as H- and D-donor, respectively (Fig. 8B–C; Fig. S15, Supporting Information). Based on these mass fragmentation analyses, a possible reaction pathway can be proposed for producing DMF from saccharides via a single-step process (Fig. 8D). Initially, an *in situ* formed acid catalyzes saccharide being converted to HMF via hydrolysis and dehydration, followed by hydrodeoxygenation over Pd NPs and PMHS to produce DMF by successively undergoing 5-methylfurfural and 5-methylfurfuryl alcohol. Notably, the hydrophobicity and Pd-support interaction of the catalyst are crucial for the effective release of acid and the sufficient access to PMHS.

4. Conclusions

In summary, a facile heterogeneous catalytic system has been developed to be highly efficient for directly producing liquid furanic/aromatic hydrocarbons (in good to excellent yields) from a variety of biomass-derived saccharides and simple bio-products, which is more pronounced than previous reports. The use of a cheap and non-toxic PMHS as reducing agent, together with readily preparative, stable and hydrophobic Pd/MIL-53(Al)-P as bifunctional catalyst, made the hydrodeoxygenation perfectly proceed under mild conditions (as low as room temperature). In addition, the Pd/MIL-53(Al)-P catalyst could be recycled for at least five times without noticeable loss in activity, and little Pd leaching into solution was detected during consecutive cycles. Deuterium isotope labeling study affirmed that the hydride transfer of PDMS assisted by Pd NPs was favorable for the domino transformations of biomass derivatives to yield furanic hydrocarbons via a single-step process. This green and highly economical catalytic protocol has the great potential to be used in industrial settings for the *in situ* domino production of furanic biofuels without intermediates separation.

Acknowledgements

This work is financially supported by Nanjing Agricultural University (68Q-0603), Postdoctoral Science Foundation of China

(2016M600422), and Jiangsu Postdoctoral Research Funding Plan(1601029A).

Appendix A. Supplementary data

Supporting Information associated with this article can be found, in the online version, at http://dx.doi.org/10.1016/j.apcatb.2017.05.039.

References

[1] J.Q. Bond, A.A. Upadhye, H. Olcay, G.A. Tompsett, J. Jae, R. Xing, D.M. Alonso, D. Wang, T. Zhang, R. Kumar, A. Foster, S.M. Sen, C.T. Maravelias, R. Malina, S.R.H. Barrett, R. Lobo, C.E. Wyman, J.A. Dumesic, G.W. Huber, Energy Environ. Sci. 7 (2014) 1500–1523.
[2] S. Crossley, J. Faria, M. Shen, D.E. Resasco, Science 327 (2010) 68–72.
[3] M.J. Climent, A. Corma, S. Iborra, Green Chem. 16 (2014) 516–547.
[4] D.D. Laskar, B. Yang, H. Wang, J. Lee, Biofuel Bioprod. Bioref. 7 (2013) 602–626.
[5] R.H. Venderbosch, ChemSusChem 8 (2015) 1306–1316.
[6] H. Li, Z. Fang, R.L. Smith Jr., S. Yang, Prog. Energy Combust. 55 (2016) 98–194.
[7] L.D. Schmidt, P.J. Dauenhauer, Nature 447 (2007) 914–915.
[8] G.H. Wang, J. Hilgert, F.H. Richter, F. Wang, H.J. Bongard, B. Spliethoff, C. Weidenthaler, F. Schüth, Nat. Mater. 13 (2014) 293–300.
[9] Y. Román-Leshkov, C.J. Barrett, Z.Y. Liu, J.A. Dumesic, Nature 447 (2007) 982–985.
[10] M. Chidambaram, A.T. Bell, Green Chem. 12 (2010) 1253–1262.
[11] A. Dhakshinamoorthy, A.M. Asiri, H. Garcia, ACS Catal. 7 (2017) 2896–2919.
[12] Z.J. Lin, J. Lu, M. Hong, R. Cao, Chem. Soc. Rev. 43 (2014) 5867–5895.
[13] A.M. Ruppert, K. Weinberg, R. Palkovits, Angew. Chem. Int. Ed. 51 (2012) 2564–2601.
[14] A. Dhakshinamoorthy, H. Garcia, Chem. Soc. Rev. 41 (2012) 5262–5284.
[15] G. Huang, Q. Yang, Q. Xu, S.H. Yu, H.L. Jiang, Angew. Chem. Int. Ed. 55 (2016) 7379–7383.
[16] K.K. Senapati, Synlett 12 (2005) 1960–1961.
[17] G. Férey, C. Mellot-Draznieks, C. Serre, F. Millange, J. Dutour, S. Surblé, I. Margiolaki, Science 309 (2005) 2040–2042.
[18] T. Loiseau, C. Serre, C. Huguenard, G. Fink, F. Taulelle, M. Henry, T. Bataille, G. Férey, Chem. Eur. J. 10 (2004) 1373–1382.
[19] H. Wu, Y.S. Chua, V. Krungleviciute, M. Tyagi, P. Chen, T. Yildirim, W. Zhou, J. Am. Chem. Soc. 135 (2013) 10525–10532.
[20] W. Zhang, Y. Hu, J. Ge, H.L. Jiang, S.H. Yu, J. Am. Chem. Soc. 136 (2014) 16978–16981.
[21] J. Yuan, X. Liu, O. Akbulut, J. Hu, S.L. Suib, J. Kong, F. Stellacci, Nat. Nanotechnol. 3 (2008) 332–336.
[22] G. Lu, S. Li, Z. Guo, O.K. Farha, B.G. Hauser, X. Qi, Y. Wang, X. Wang, S. Han, X. Liu, J.S. DuChene, H. Zhang, Q. Zhang, X. Chen, J. Ma, S.C.J. Loo, W.D. Wei, Y. Yang, T.J. Hupp, F. Huo, Nat. Chem. 4 (2012) 310–316.
[23] P.S. Ho, G.W. Rubloff, J.E. Lewis, V.L. Moruzzi, A.R. Williams, Phys. Rev. B 22 (1980) 4784–4790.
[24] A.Y. Stakheev, W.M.H. Sachtler, J. Chem. Soc. Faraday Trans. 87 (1991) 3703–3708.
[25] B. Chen, F. Li, Z. Huang, G. Yuan, Appl. Catal. B: Environ. 200 (2017) 192–199.
[26] A.J. Kumalaputri, G. Bottari, P.M. Erne, H.J. Heeres, K. Barta, ChemSusChem 7 (2014) 2266–2275.
[27] M.Y. Chen, C.B. Chen, B. Zada, Y. Fu, Green Chem. 18 (2016) 3858–3866.
[28] B. Saha, C.M. Bohn, M.M. Abu-Omar, ChemSusChem 7 (2014) 3095–3101.
[29] M. Chidambaram, A.T. Bell, Green Chem. 12 (2010) 1253–1262.
[30] A.S. Nagpure, N. Lucas, S.V. Chilukuri, ACS Sustain. Chem. Eng. 3 (2015) 2909–2916.
[31] Y. Zu, P. Yang, J. Wang, X. Liu, J. Ren, G. Lu, Y. Wang, Appl. Catal. B: Environ. 146 (2014) 244–248.
[32] A. Volkov, K.P.J. Gustafson, C.W. Tai, O. Verho, J.E. Bäckvall, H. Adolfsson, Angew. Chem. Int. Ed. 54 (2015) 5122–5126.
[33] H. Li, Z. Fang, J. He, S. Yang, ChemSusChem 10 (2017) 681–686.
[34] H. Li, W. Zhao, A. Riisager, S. Saravanamurugan, Z. Wang, Z. Fang, S. Yang, Green Chem. 19 (2017) 2101–2106.
[35] M.J. Gilkey, P. Panagiotopoulou, A.V. Mironenko, G.R. Jenness, D.G. Vlachos, B. Xu, ACS Catal. 5 (2015) 3988–3994.